Research Square

Preprints are preliminary reports that have not undergone peer review. They should not be considered conclusive, used to inform clinical practice, or referenced by the media as validated information.

Monitoring high-temperature sensor with optical performance in Terahertz Using graphene in power plant industries

Hadi Sharifi

h.sharifi97ms@gmail.com

University of Tabriz

Omid Mohsen Daraei

University of Houston

Ali Pourziad

University of Tabriz

Mohammad Bemani

University of Tabriz

Research Article

Keywords: graphene, nanotechnology, optical sensor, high temperature, terahertz

Posted Date: August 29th, 2023

DOI: https://doi.org/10.21203/rs.3.rs-3283837/v1

License: This work is licensed under a Creative Commons Attribution 4.0 International License. Read Full License

Additional Declarations: No competing interests reported.

Abstract

Optical sensors getting widespread usage in almost every field, especially industries. A high thermal optical sensor is proposed to predict and prevent the environmental temperature in power plants. A high sensitivity, accuracy, low cost, compact size, linear operation, and suitable transmission coefficient optical sensor in a wide thermal range is achieved that changing the surrounding temperature has a severe effect on the conductivity of graphene which changes the transmission power of the sensor. In this article, the position of the graphene sheet affects the interaction of light and graphene, effectively. The Cylindrical diameter of the optical sensor is 4.1 lambda which is the smallest in size among the references checked and has the desired performance from room temperature to 2000 degrees Kelvin, indicating the suitable efficiency of the sensor and the fiber optic sensor with graphene coating has great potential in the field of measurement, especially in the temperature of the surrounding atmosphere in the industry.

I. Introduction

Graphene is two-dimensional carbon material with low thicknesses and extremely high mobility in the atom size arranged in a honeycomb crystal lattice that can be used for sensing applications.[1, 2]. The use of three σ-electrons in carbon-carbon bonding results in a system of delocalized π-electrons perpendicular to the honeycomb plane giving rise to exceptional electrical properties of graphene. Graphene is one of the most important substances especially in optical engineering over the last years.[3] Ease of use in various types of applications such as medical sensors (blood component and diseases), physical sensors (strain, pressure, temperature, humid), and chemical sensors (oil, gas) enable researchers to overcome the difficulties of electrical and electronic sensors like large size, large weight, instability, power loss, leakage current, vulnerable to the hazardous environment and other problem[4, 5]

One of the most important sensors among all other sensing strategies is the optical fiber sensor which has achieved a high impact in the last decades. These sensors offer several advantages over electronic sensors, additionally, optical fiber sensors are light and small, resistant to harsh environments and high temperatures. Also, biocompatible, immune to electromagnetic fields, and electromagnetically passive. They are especially suitable for some specific applications, such as biosensing health and medicine applications[6–8], offshore applications, and sensing in harsh and flammable environments[9]. As a consequence, the unique optical, chemical, and morphological properties of graphene combined with the benefits of optical fiber sensing schemes are attracting a growing interest in the scientific community. Until now, not only publications on optical fiber sensors based on graphene materials are limited, but the increase in the number of publications observed in the last few years is a clear indication of this fact.[10–12]. Industries like sugar mills, oil refineries, power, chemical, and many other industries require a boiler for a specific operation. The primary operation of the boiler is to generate steam for various process operations or applications mainly used in the heating application.[13, 14]

A soft sensor was introduced to predict the oxygen content of the steam boiler flue gas in a gas-fired boiler system [15]. In [16] a soft sensor measuring oxygen content in flue gases at an oil refinery using a Zirconia oxygen analyzer was offered and later in [4], the sensitivity of 4.7 pm/$^{\circ}\mathrm{C}$ was obtained by the tapered PCF (Photonic Crystal Fiber) in a range of T = 20$^{\circ}\mathrm{C}$ to T = 930$^{\circ}\mathrm{C}$. Four fiber sensors were dropped into a heated furnace to simulate a step transient in temperature from room temperature to various final temperatures of 700–1100 $^{\circ}\mathrm{C}$ [17].

In [1] a highly thermal conductive polymer of graphene composites with rapid room-temperature self-healing capacity ($13 \pm 0.2 Wm^{-1}K^{-1}$) was proposed and a wireless graphene-based thermal patch for obtaining temperature distribution and performing thermography was used in [18]. In [19] a magnetic field and temperature monitoring from 25°C to 60°C by wireless multifunctional surface wave sensor was proposed. As in [20] a high sensitivity with linear operation suitable transmission coefficient temperature sensor based on FBG (Fiber Bragg Grating) with a cover of graphene simulated and designed for 300–500 K. In [21] mechanism and behavior of an electrochemical sensor were examined to work in a combustion boiler, due to demanding operational temperatures of more than 1000$^{\circ}\mathrm{C}$. (range of 1000–1200 $^{\circ}\mathrm{C}$).

In this paper, a high temperature sensor for using in industries is presented, and in the next sections the structure of biosensor, the properties of graphene and the simulations of Finite Integration Technique with the commercial CST STUDIO SUITE package is presented. Also, the simulation parameters, the comparative studies and the conclusion part is mentioned in the next sections.

II. Experimental setup

In this paper graphene film with a lower refractive index is transferred from silica substrate to MgF_2 substrate. CST simulation structure by using a Graphene ribbon is shown in Fig. 1. The microfiber is closely absorbed into the graphene film due to the presence of a high peak field and electrostatic force between them. Because the conductive band and capacity band meet at two points, a relationship of energy dispersion and linear motion can be seen in the vicinity of Dirac points and carries behavior that can be modeled as Dirac fermions without mass, and only transmission between bands is allowed. The Kubo formula can be used to describe the dynamic response of graphene, including the inter-band and intra-band as in [20]

$$\sigma = \sigma_{\mathrm{int}\,er} + \sigma_{\mathrm{int}\,ra}$$

1

$$\sigma = \sigma_{\mathrm{int}\,ra} + \sigma'_{\mathrm{int}\,er} + \sigma''_{\mathrm{int}\,er}$$

2

$$\sigma_{\mathrm{int}\,ra} = \sigma_0 \frac{4\mu}{\pi} \frac{1}{\hbar\tau_1 - i\hbar\omega}$$

3

$$\sigma'_{\text{inter}} = \sigma_0(1 + \frac{1}{\pi}\arctan\frac{\hbar\omega - 2\mu}{\hbar\tau_2} - \frac{1}{\pi}\arctan\frac{\hbar\omega + 2\mu}{\hbar\tau_2})$$

4

$$\sigma''_{\text{inter}} = -\sigma_0\frac{1}{2\pi}\ln\frac{(\hbar\omega + 2\mu)^2 + \hbar^2{\tau_2}^2}{(\hbar\omega - 2\mu)^2 + \hbar^2{\tau_2}^2}$$

5

In the above relationships, $\sigma_0 = \frac{e^2}{4\hbar} = 60.85(\mu s)$is the overall conductivity of graphene, e is the electron load, the $\hbar$is the Planck constant and $\tau$is dispersion time. The inter-band and intra-band transmission is related to the μ (chemical potential) and ω (the angular frequency) of incident light. When μ = 0, no intra-band transfer will occur. When |μ|< $\frac{\hbar\omega}{2}$ (slightly n-doped or p-doped) optical transmission is influenced by inter-band transmission. In n- and p-doped graphene (related to positive and negative gate voltage), incidental photons with energy less than cannot be absorbed. This is because electron states are filled in the conductive band.

Figs. 2 & 3 show graphene's surface conductivity and permittivity as a function of chemical potential at λ = 1550 nm, and T = 300K, respectively.

In the structure, off-screen conductivity $\sigma_\perp$ can be in-screen conductivity $\sigma_\parallel$ and using the graphene as an analytical expression derived from random phase approximation because of no ENZ (Epsilon Near Zero) effect for optical conductivity of graphene as in [20, 22]:

$\sigma_\parallel = \frac{i8\sigma_0}{\pi}\frac{E_{th}}{E_{ph}+iE_s}\ln\left[2\cos\left(\frac{E_F}{2E_{th}}\right)\right] + \sigma_0\left[\frac{1}{2} + \frac{1}{\pi}\tan^{-1}\left(\frac{E_{ph}-2E_F}{2E_{th}}\right)\right]$ + $\sigma_0\left[-\frac{i}{2\pi}\ln\frac{(E_{ph}+2E_F)^2}{(E_{ph}-2E_F)^2+4{E_{th}}^2}\right]$ (6)

In (6), $E_{th} = K_BT$(K_B is Boltzmann constant, T is the temperature) and, E_F is fermi energy (i.e the chemical potential of μ_c) in eV, $E_{ph} = \frac{hc}{\lambda}$is photon energy in eV (h is the Planck constant), and is energy dispersed in eV for dispersion time τ.

III. Results and discussions

After putting graphene strips on the MgF_2substrate of microfiber, it makes it possible to create a surface plasmon mode that can be emitted or prevented from propagation due to the bias voltage applied to surface plasmon waves graphene. In Table 1 simulation parameters by the FIT numerical method can be seen.

TABLE I. Simulation parameters

parameter	Parameter list	
	Expression	*Value*
Microfiber	diameter	6μm
Graphene	Coat thickness	0.2μm
	Relax time	0.2ns
	Chemical potential	0.4eV
MgF_2	Substrate epsilon	2
	Substrate width	12μm
	Substrate height	6μm
wavelength	Center	189.8 THz

From complex optical conductivity, the complex dielectric constant of graphene $\varepsilon_{\parallel}\left(\mu_c\right)$ is calculated from the following relationship as in [20]:

$$\varepsilon_{\parallel}\left(\mu_c\right) = 2.5 + \frac{j\sigma_0\left(\mu_c\right)}{\omega\varepsilon_0 d_G}$$

7

Above, $d_G = 0.7nm$is single-layer graphene thickness, $\omega$and is the overall conductivity of graphene, the chemical potential, the frequency of incident light, and the permittivity of free space, respectively. In Fig. 4 the results of optical sensor simulation for the real and imaginary part of the surface conductivity of graphene in various temperatures, are shown. As seen in previous sections, the infrared spectral limit has been highly considered for the study of plasmonic devices due to their integrity with electronic devices and the possibility of designing devices with active control of surface plasmon resonance in the common metal-dielectric elements. However, due to low refractive index changes by applying voltage, mechanical force, or temperature, plasmonic devices have disadvantages such as high-power consumption, low switching speed, and other problems.

In Fig. 4, it is obvious that the real part of the surface conductivity of graphene is constant after a frequency of 210THz for any thermal variations, but there is a big difference in the vicinity of 150THz frequency for any thermal changes. Moreover, huge differences are seen in Fig. 5 for the imaginary part of the surface conductivity of graphene, however, after the range of 210THz frequency, the curve is getting linear and there are no changes for thermal variations after that frequency. Figure 6 shows the reflection coefficient and Fig. 7 shows the transmission coefficient of the optical sensor in CST software, respectively.

As can be seen, the optical sensor has a fuzzy shift for 1000K-1500K and 2000K and shows good performance and high sensitivity which is useful for controlling high temperature and fire prevention in an industrial environment, especially Thermal power plants, Refineries, Electrical power plants, and other Professions. By considering the aforementioned principle, this attempt could be implemented for industrial applications. Table II shows the comparison of this work and recently published reports. By comparing this work and the other five recent works, it is clearly shown that this work has a wide range of detection among the other sensors. Also, the size of the Cylindrical structure diameter of the biosensor is 4.1 lambda for the proposed sensor which is the smallest among the references[2] which has 5.25 lambda, and [4] which has 4.35 lambda.

TABLE II.Comparative study between the proposed biosensor and recently published reports

References	Detection Range	Sensor Type	Detection parameter
McCary, K.M., et al (2014)	700°C to 1100°C	Type-I, type-II SMF-28 FBGs	Temperature sensing
Yu, H., et al (2022)	25°C to 800°C	Polymer/Graphene Composite	Thermal conductive self-healing
Sanusidin, S., et al (2018)	20°C to 930°C	Photonic Crystal Fiber	High-Temperature sensing
Behera, C., et al (2022)	0°C to 1200°C	Oxygen analyzer in Boiler	Temperature, pressure, steam, and water flow
Sina Javanshir, et al (2018)	350 K to 400 K	Micro ring resonator	Micro temperature sensor
This work	300 K to 2000 K	Optical sensor	High-Temperature sensing

IV. Conclusion

In this paper, the optical sensor has the desired performance from room temperature to 2000 degrees Kelvin, indicating the suitable efficiency of the sensor and the fiber optic sensor with graphene coating has great potential in the field of measurement, especially in the temperature of the surrounding atmosphere. The position of the graphene sheet in the fiber optic has an enormous effect on the interaction between input light and graphene. The physical phenomena in the structure is using the thermal feature and surface conductivity of graphene for detecting the environment temperature and graphene material was used in the optic sensor.

Declarations

Acknowledgment

The authors would like to thank Dr. Ehsan Khodapanah from Faculty of Electrical & Computer Engineering Department at University of Tabriz for his motivation and efforts.

Conflicts of interest

The authors have no competing interests as defined by Springer, or other interests that might be perceived to influence the results and/or discussion reported in this paper.

Ethical Approval

This article does not contain any studies with human participants or animals performed by any of the authors.

Authors' contributions

All authors contributed equally to this work.

Availability of data and materials

Data used/generated during the current study are available from the corresponding author on reasonable request.

Funding

There is no funding to this work.

References

1. Yu, H., et al., *Highly Thermally Conductive Polymer/Graphene Composites with Rapid Room-Temperature Self-Healing Capacity.* Nano-Micro Letters, 2022. **14**(1): p. 135.
2. Sina Javanshir , A.P., Saeed Nikmehr, *Optical Temperature Sensor with Micro Ring Resonator and Graphene to reach High Sensitivity.* optik, 2018.
3. Lu, P., et al., *Distributed optical fiber sensing: Review and perspective.* Applied Physics Reviews, 2019. **6**(4): p. 041302.
4. Sanusidin, S., et al. *High Temperature Sensor Based on Tapered Few Modes All-Solid Photonic Bandgap Fiber*. in *2018 IEEE 7th International Conference on Photonics (ICP)*. 2018. IEEE.
5. Ma, S., et al., *Highly sensitive terahertz sensor based on graphene metamaterial absorber.* Optics Communications, 2023. **528**: p. 129021.
6. Eskandari, S., et al. *Design and Performance Analysis of a Novel Optical Biosensor for Measuring Glucose Concentration in Urine*. in *2022 30th International Conference on Electrical Engineering (ICEE)*. 2022.

7. Zamzam, P., et al., *Graphene-based polarization-insensitive metamaterials with perfect absorption for terahertz biosensing applications: Analytical approach.* Optics & Laser Technology, 2023. **163**: p. 109444.
8. Norouzi Razani, A., et al., *Absorption-based ultra-sensitive RI sensor based on the flower-shaped graphene resonator for early detection of cancer.* Optics Communications, 2022. **524**: p. 128775.
9. Saini, R., et al., *Analysis of graphene coated optical fiber for visible range refractive index sensing.* Optics Communications, 2023. **529**: p. 129097.
10. Miguel, H., et al., *Optical Fibre Sensors Using Graphene-Based Materials: A Review.* MPDi, 2017. **17**(155).
11. Zhang, H., et al., *Graphene-enabled wearable sensors for healthcare monitoring.* Biosensors and Bioelectronics, 2022. **197**: p. 113777.
12. Hoffmann, L., et al., *Applications of fibre optic temperature measurement.* Estonian Journal of Engineering, 2007. **13**(4).
13. Behera, C., et al., *Control and analysis of crucial parameters for an automatic boiler unit in a chemical industry.* International Journal of Engineering, Science and Technology, 2022. **14**(3): p. 94-103.
14. Chicherin, S., et al. *Controlling Temperatures in Low-Temperature District Heating: Adjustment to Meet Fluctuating Heat Load*. in *XIV International Scientific Conference "INTERAGROMASH 2021"*. 2022. Cham: Springer International Publishing.
15. Effendy, N., et al., *The prediction of oxygen content of the flue gas in a gas-fired boiler system using neural networks and random forest.* IAES Int J Artif Intell (IJ-AI), 2022. **11**(3): p. 923-929.
16. Kurniawan, E.D., et al., *Soft sensor for the prediction of oxygen content in boiler flue gas using neural networks and extreme gradient boosting.* Neural Computing and Applications, 2022.
17. McCary, K.M., et al., *Response of Distributed Fiber Optic Temperature Sensors to High-Temperature Step Transients.* IEEE Sensors Journal, 2018. **18**(21): p. 8755-8761.
18. Kang, M., et al., *Wireless graphene-based thermal patch for obtaining temperature distribution and performing thermography.* Science Advances. **8**(15): p. eabm6693.
19. Yang, Y., et al., *Wireless Multifunctional Surface Acoustic Wave Sensor for Magnetic Field and Temperature Monitoring.* Advanced Materials Technologies, 2022. **7**(3): p. 2100860.
20. Hadi Sharifi, A.P., Mohammad Bemani, *Nano Optical Temperature Sensor based on Fiber Bragg Grating using Graphene.* Results in Optics, 2022.
21. Wang, Y., et al., *NiO-based sensor for in situ CO monitoring above 1000 °C: behavior and mechanism.* Advanced Composites and Hybrid Materials, 2022. **5**(3): p. 2478-2490.
22. Jia, W., et al., *Dynamically tunable optical properties in graphene-based plasmon-induced transparency metamaterials.* Chinese Physics B, 2019. **28**(2): p. 026102.

Figures

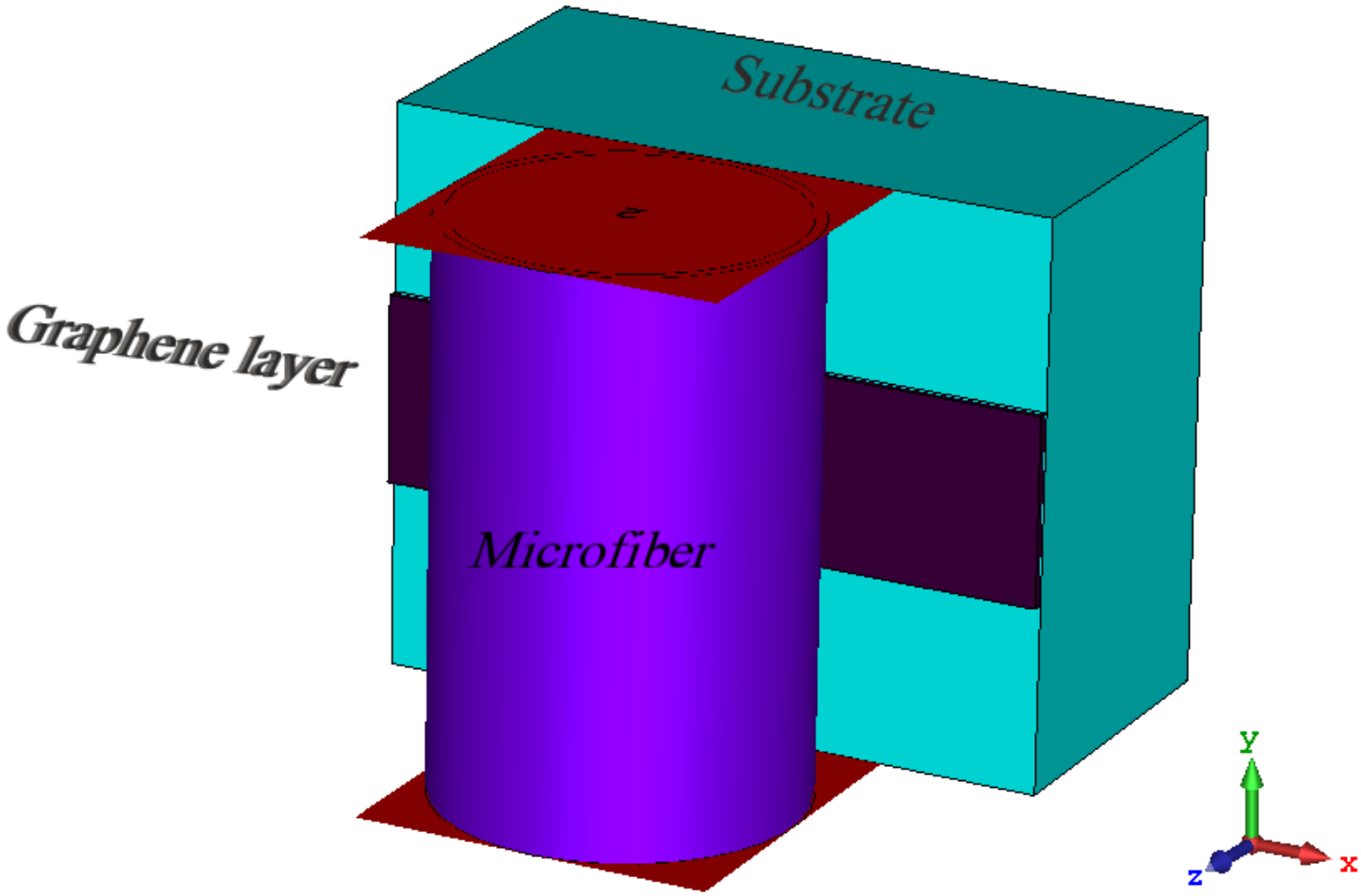

Figure 1

Structure of the proposed optical sensor

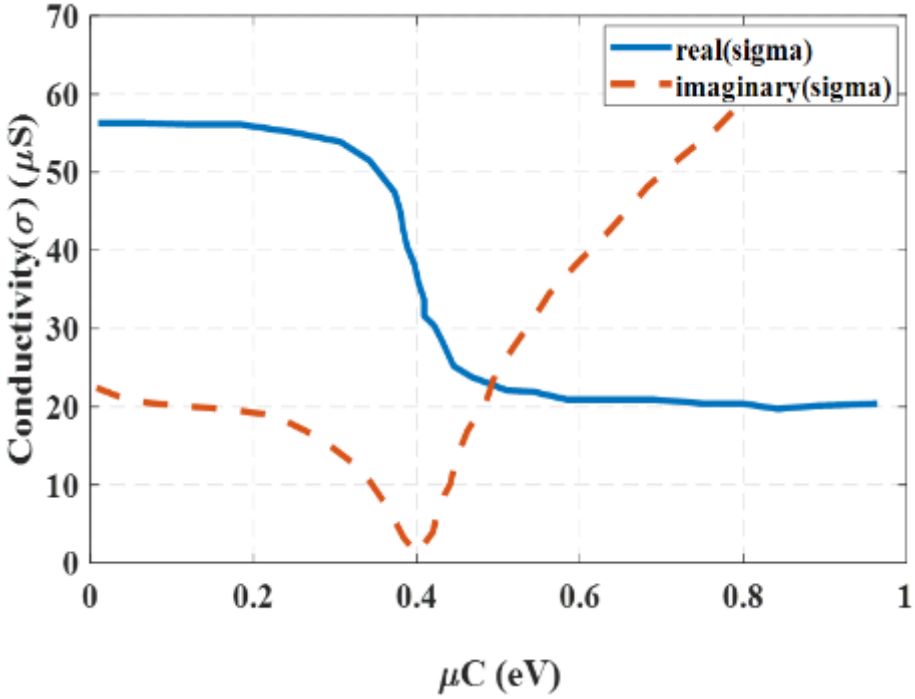

Figure 2

Surface conductivity Vs Chemical potential

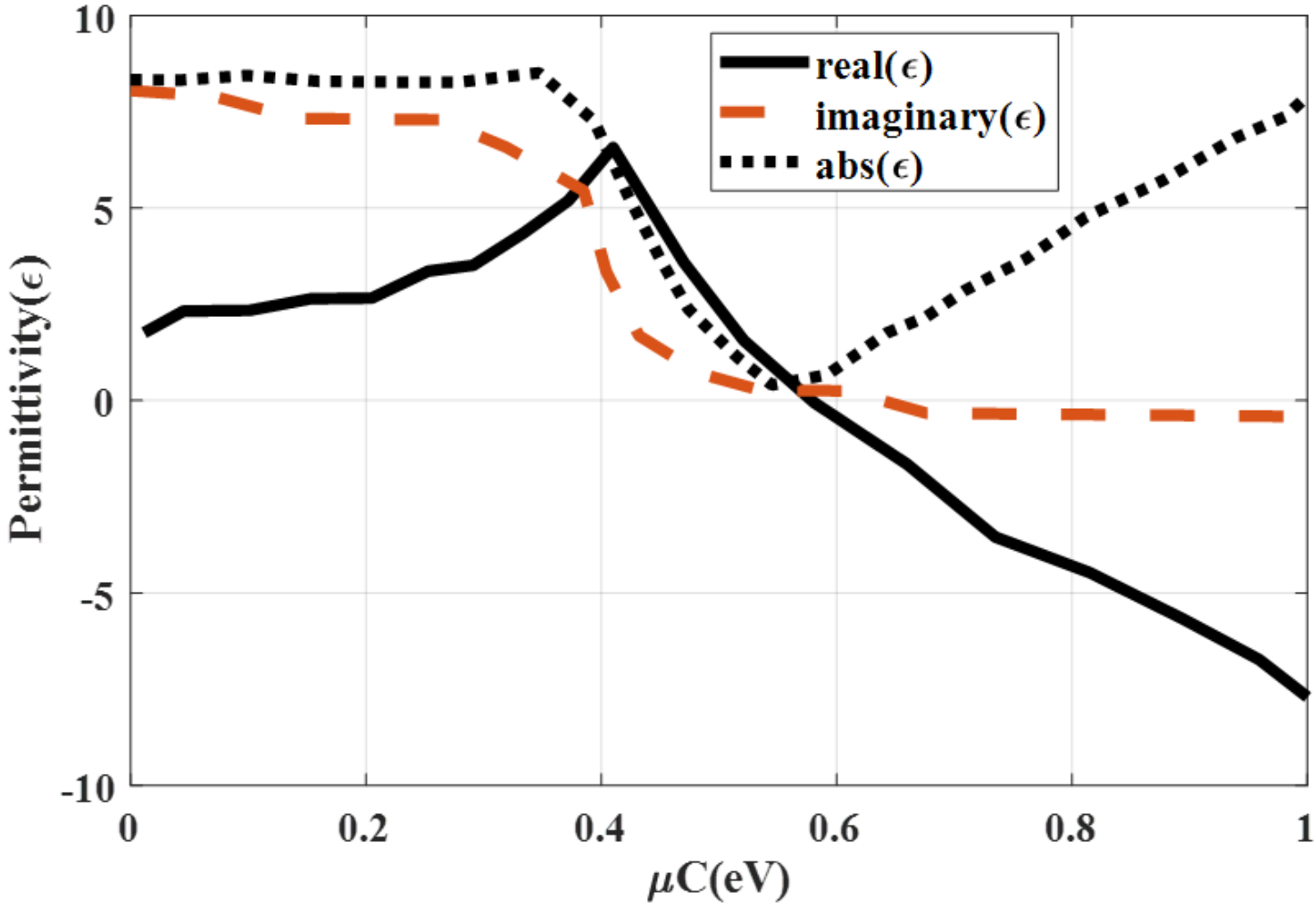

Figure 3

Permittivity of graphene Vs Chemical potential

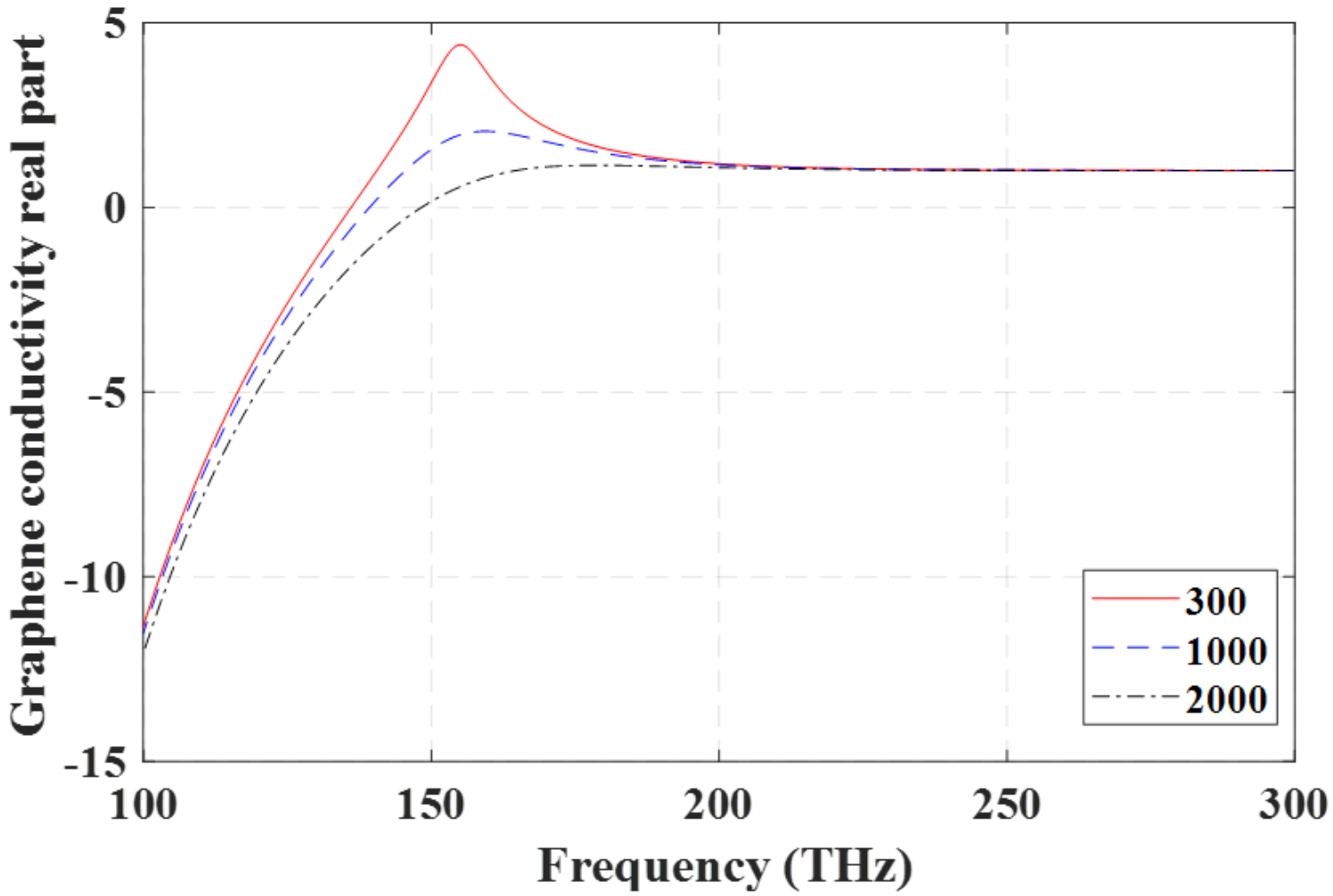

Figure 4

Real part of the surface conductivity of graphene

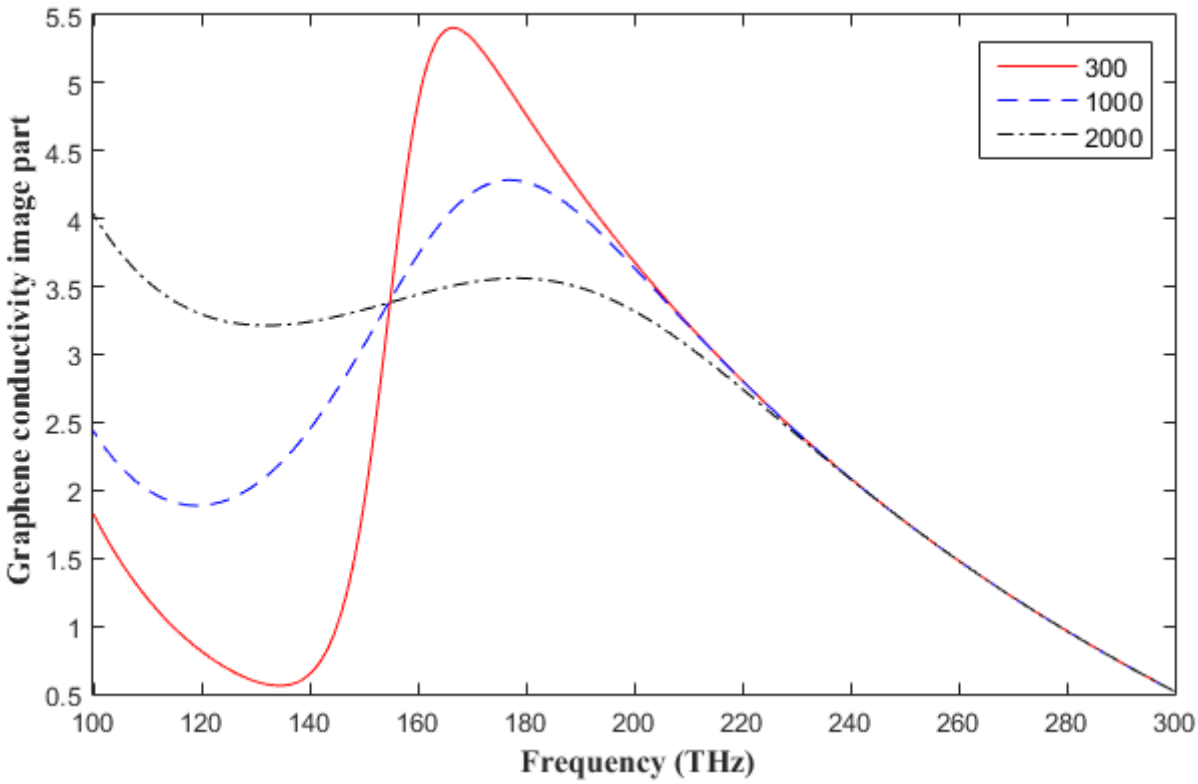

Figure 5

Imaginary part of the surface conductivity of graphene

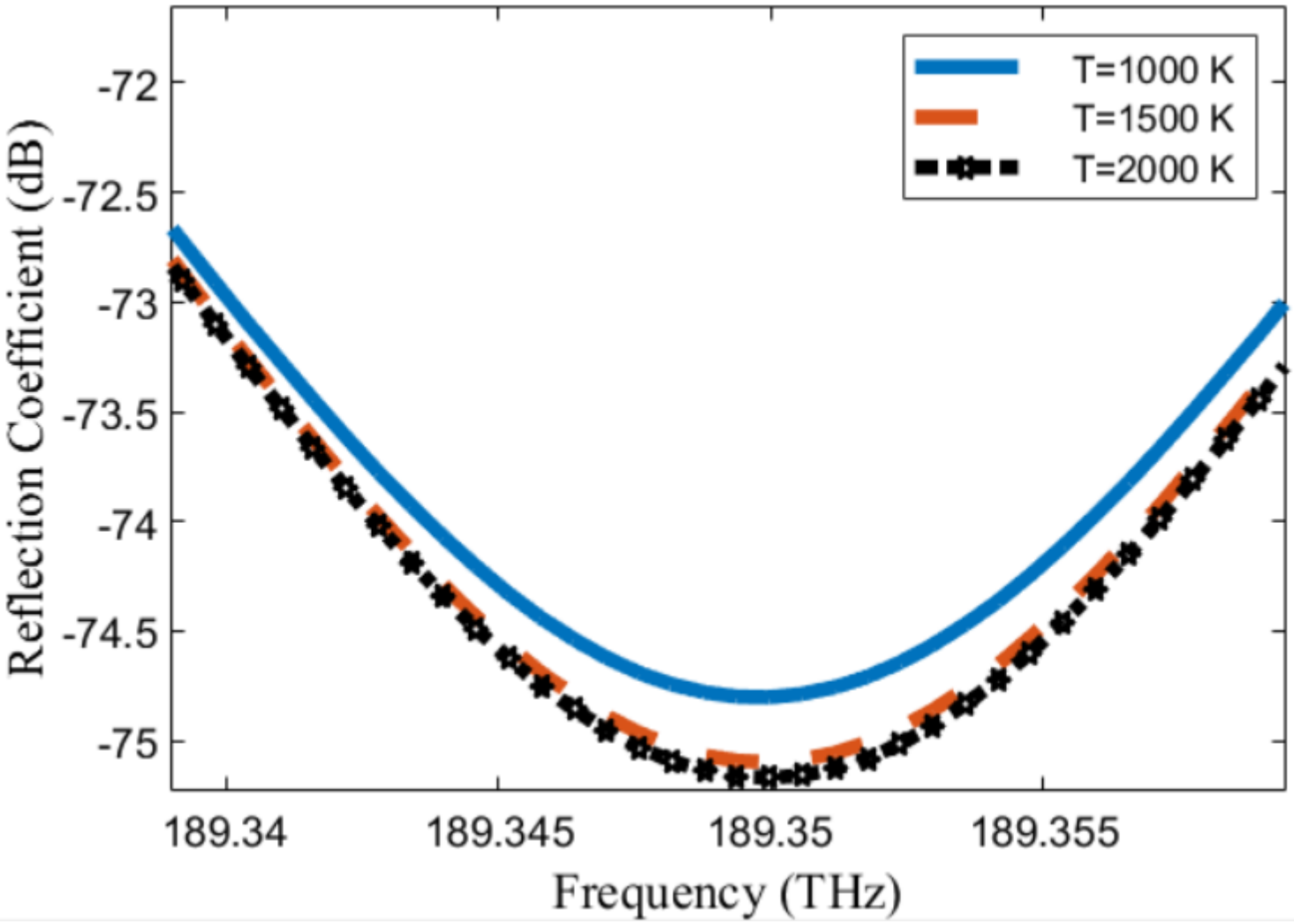

Figure 6

Reflection coefficient of the optical sensor

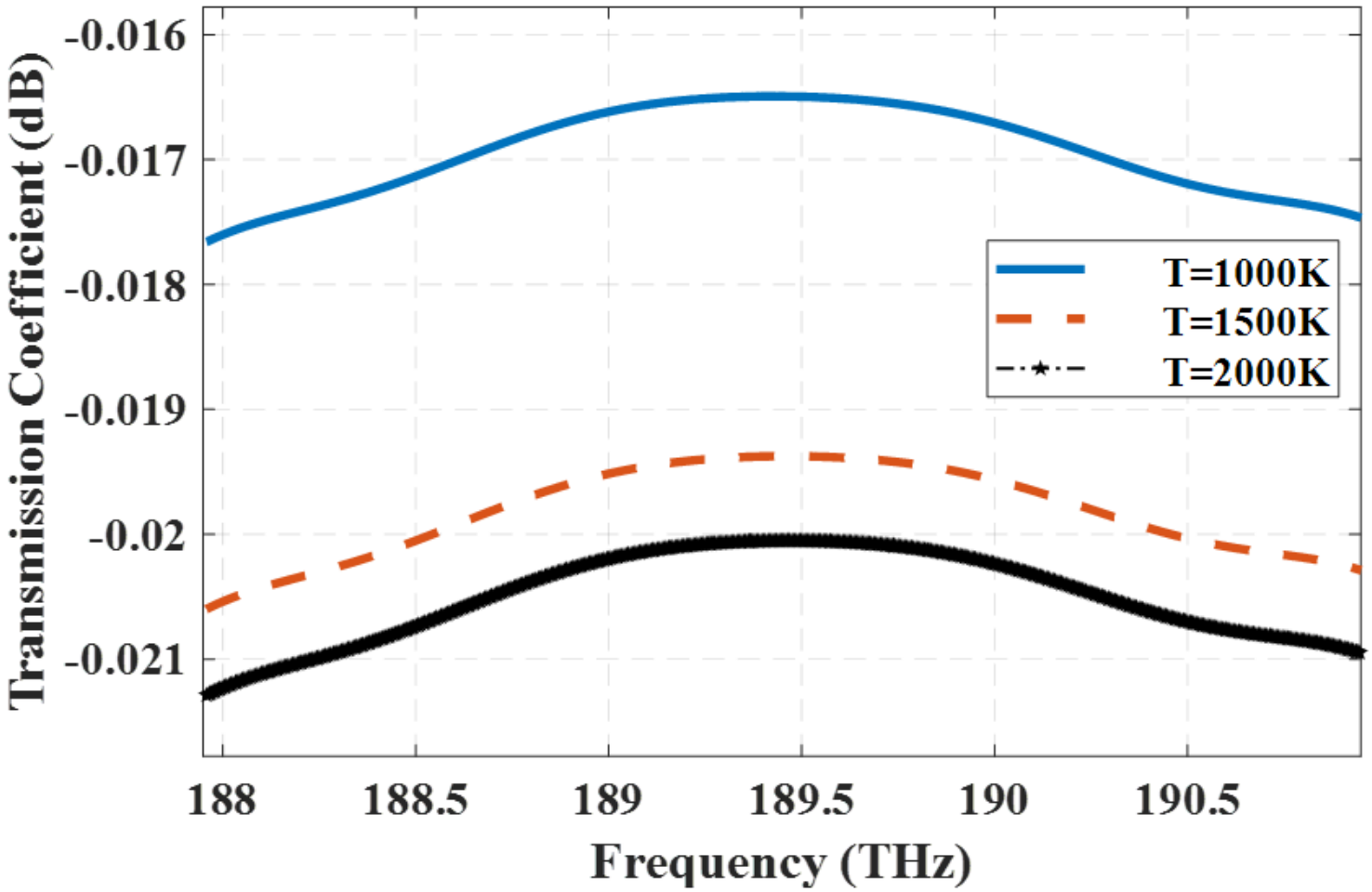

Figure 7

Transmission coefficient of the optical sensor